Nonlinear Ionization of Organic Molecules in High Intensity Laser Fields

S. M. Hankin,* D. M. Villeneuve, P. B. Corkum, and D. M. Rayner

Femtosecond Science Program, Steacie Institute for Molecular Science, National Research Council, 100 Sussex Drive, Ottawa, Ontario, Canada K1A 0R6

(Received 8 November 1999)

We use a series of 23 organic molecules to study ionization of complex media caused by their interaction with intense 40 fs, 0.8 μm pulses. All molecules reach saturated ionization at higher intensities than would be expected for atoms of the same ionization potential, reminiscent to what has been reported for dielectric breakdown with femtosecond pulses. Dependence of the ionization rate on the alignment of the molecule with the laser field is ruled out as the cause of the high saturation intensities. All molecules allow a significant range of intensities between the region of approximately 100% ionization and before the second and subsequent electrons are removed.

PACS numbers: 33.80.Rv, 82.50.Fv

Using rare gas atoms, two limits of nonlinear atomic ionization are well explored. When only a few photons are involved in ionization, the ionization rate is described by perturbation theory. This limit is usually referred to as the multiphoton ionization limit [1]. When the number of photons is very large, ionization can be described as tunneling. The most successful theory for determining the ionization rate in this limit is known as the Ammosov-Delone-Krainov (ADK) tunneling theory [2].

Computer simulations using the single active electron approximation study the intermediate region. They provide impressive agreement with experiment in helium over many orders of magnitude and confirm a widely held assumption that tunneling rates provide a lower bound on the ionization rate [3]. That is, corrections will only *add* to the tunneling rate and tunneling provides a realistic (but lower bound) estimate of femtosecond ionization rates for high ionization potential atomic gases. This lower bound is frequently used as a reference rate and is called the ADK rate.

Strong field processes are implicated in many areas of science. For example, strong fields near the tip of a scanning tunneling microscope lead to the local tunneling that results in the atomic scale resolution [4]. The strong fields associated with ultrashort laser pulses play an important role in laser machining [5] and in high harmonic generation [6]. They promise a novel approach to chemical dynamics through time-resolved Coulomb explosion imaging [7] and may have an impact as universal and highly efficient ionization sources for analytical mass spectrometry [8]. However, compared with rare gas atoms, much less quantitative research has been performed on complex media.

Our aim is to study systematically whether and how the ideas from atom ionization extend to complex media. Initially we ask if they are easier or harder to ionize than "virtual rare gas atoms" of the same ionization potential and are there any global trends with increasing complexity. Molecules of increasing size in the gas phase allow us to use the quantitative experimental methods of atomic physics to address these issues.

The atomic tunneling model provides a good qualitative understanding of the DC field ionization of molecules in field ionization mass spectrometry experiments [9]. More recent experience with atomic laser ionization suggests that the relatively low ionization potentials of molecules, their lower lying excited states, and their larger size will each contribute to an increase in the ionization rate over the reference ADK atomic rate. In particular, a recent quasistatic model based on the extended range of molecular potentials predicts this [10]. For the 23 molecules that we study, our only selection criterion is that we avoid structures where multielectron resonances [11] may play a role. We find higher-than-ADK saturation intensities for all molecules that we have studied, some by almost a factor of 5.

Our method allows us to address indirectly whether the ionization rate changes with the alignment of the molecular axes with the laser polarization. There has been a great deal of discussion on the alignment sensitivity to strong field femtosecond laser ionization [10,12–14] based on model calculations. Furthermore, it is well known that ionization of dissociating molecular ions is very sensitive to alignment [15]. Our results provide no evidence for alignment sensitivity of the tunneling rate for neutral molecules.

The ionization experiments were carried out in a single-stage time-of-flight (TOF) mass spectrometer. Differential pumping allowed the TOF source chamber to be operated at up to 10^{-5} Torr, while maintaining the flight chamber at high vacuum. A 0.5 mm slit at the entrance to the drift region, orthogonal to the laser beam and the TOF axis collected ions produced only at the center portion of the laser focal volume. A Raleigh length of $\sim$3 mm ensured that ions were collected only from a region of cylindrical geometry [16].

A Ti:sapphire laser system delivered 44 fs FWHM, 800 nm pulses with maximum energy of 350 μJ. We used a rotatable half wave plate followed by a polarizer as a variable attenuator. This was placed before the final

 0031-9007/00/84(22)/5082(4)$15.00

grating compressor to avoid nonlinear interactions with the wave plate or polarizer.

The beam was focused using a 260 mm f.l. lens to a 27 μm diameter waist at I_0/e [measured using a charge coupled device beam-profiling camera]. The maximum intensity, calculated from measurements of the energy and beam profile and confirmed by comparing the observed helium ionization intensity dependence, was 1×10^{15} W cm^{-2}.

The ionization signal S, produced by a parallel Gaussian beam of peak intensity I_0, is given by

$$S = \alpha \pi R^2 c l \phi \int_0^{I_0} \frac{1 - e^{-W(I)\tau}}{I} dI, \qquad (1)$$

where α is the instrument sensitivity, R is the radius of the beam at I_0/e, c is the concentration of neutrals, and l is the length of the cylinder projected on the detector. ϕ is the ionization branching ratio compared to neutral pathways such as dissociation and is taken here to be independent of I. $W(I)$ is the intensity dependent ionization rate and τ is the effective width of the laser pulse [17]. As long as $W(I)$ increases with I, the dependence of S on I_0 takes the form shown in Fig. 1. In the high intensity limit, where $\exp[-W(I) \ll 1]$, Eq. (1) implies

$$S = \alpha \pi R^2 c l \phi [\ln(I_0) + \ln(I_{\text{sat}})], \qquad (2)$$

so that the slope of the plot of S vs $\ln(I_0)$ tends to a limiting value of $\alpha \pi R^2 c l \phi$. This limiting slope is independent of the form of $W(I)$ but includes all the experimental factors required to calibrate the experiment using rare gas ionization. With the proviso that α is not species dependent and c is known this leads to absolute ion yields. We determined c by introducing the sample gas through a leak valve, at a predetermined dilution of between 1% and 5% in He buffer gas. The dilution in He also ensured that the gas dependence of the ion gauge response did not significantly distort the pressure measurements. We compared the ionization of He, Ne, and Xe to show that α is independent of the mass of the ion, at least for atoms in the range 4–140 amu, at fixed acceleration voltage and multichannel plate detector bias. Individual ion signals (or the envelope of adjacent ion signals) were recorded as a function of laser intensity using an array of five boxcars. Four percent of the laser beam was split off to measure the laser pulse energy. Each run involved $\sim 10^5$ laser shots spread over the intensity range under study.

Figure 2 shows experimental ionization data for Xe and benzene. They have the same form as predicted by Eq. (1) and as shown in Fig. 1. The Xe curve, where it is

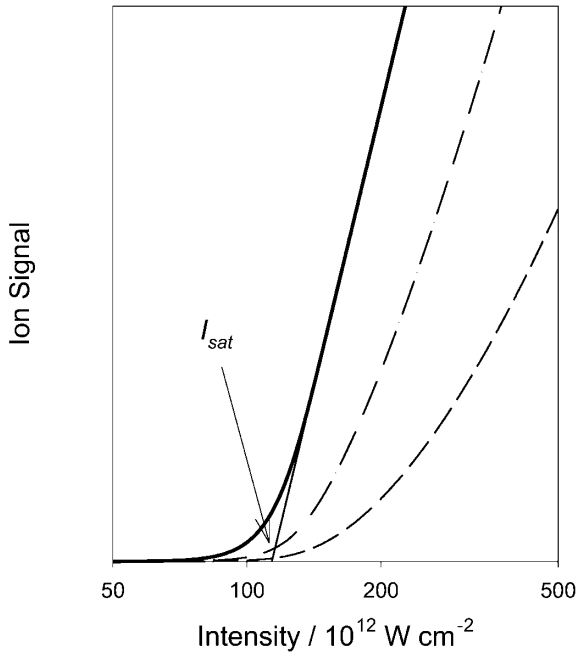

FIG. 1. Dependence of intense field laser ionization on intensity under parallel beam irradiation conditions. The solid line shows the behavior predicted when the ionization rate is modeled by a multiphoton mechanism, $[W(I) = I^{\sigma n}]$, with $n = 8$ and $\sigma = 10^{-99}$ W^{-n}cm^{2n} s^{-1} for a 20 fs square temporal pulse. The other two curves show how, for molecular ionization, sensitivity to the alignment of the electric field with a particular molecular axis would alter the predicted behavior. The dashed line is for the limiting case where only one axis of the molecule is active; the dash-dotted line is for the intermediate case where two orthogonal axes are active.

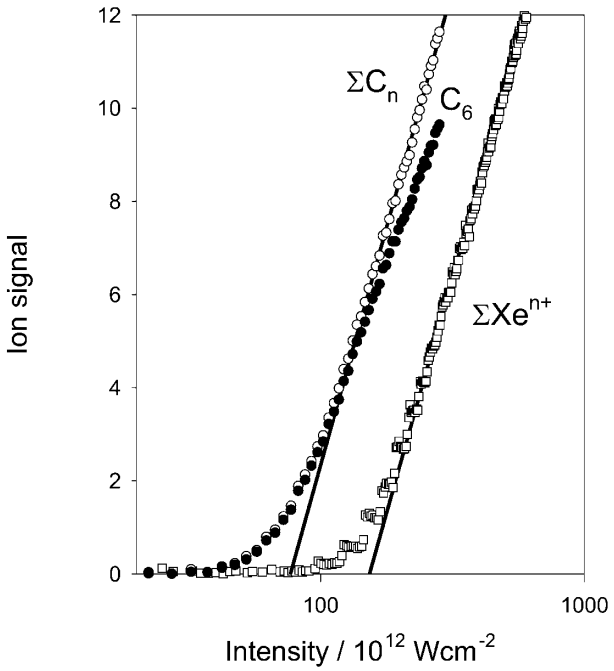

FIG. 2. Intensity dependence of the femtosecond laser ionization of xenon and benzene. The open squares refer to the total Xe ion yield, arrived at by summing the singly, doubly, and triply charged ion signals. The filled circles show the behavior of the benzene parent C_6 ion. The open circles show the total ion signal following the onset of limited postpulse ion fragmentation at higher intensities. Ion signals have been normalized to the partial pressures of Xe and benzene. The solid lines are fits to the high intensity linear portions of the data.

certain that $\phi = 1$ and that there are no alignment effects, calibrates the experiment. The curves for Xe and benzene are remarkably similar apart from a shift in the intensity axis. As the benzene curve reaches the same limiting slope we conclude that ϕ is also 1 in the case of benzene. This demonstrates that we can achieve 100% efficient ionization of an organic molecule over an appreciable range of intensity before Coulomb explosion sets in. However, at high intensity (for benzene $\sim 2.25 \times 10^{14}$ W cm^{-2}) we observe deviation from the limiting slope. At this intensity the ionization dynamics suddenly become much more complex. We see the appearance of atomic fragments in the mass spectrum, a broadening of mass spectrum peaks indicating fragments with high translational energy and a reduction in the ion collection efficiency due to translational energy orthogonal to the TOF axis. We attribute the deviation to the Coulomb explosion of the molecule.

The total ion yield intensity dependence curve for benzene in Fig. 2 is representative for all the molecules studied. Within error, all reach the same limiting slope and have the same asymptotic behavior as Xe. All show a region of at least a factor of 2 between saturated ionization and catastrophic ionization leading to Coulomb explosion. Below the Coulomb explosion threshold we measure the total ion yield as the sum of parent and fragment ions to take unimolecular decomposition following ionization into account.

Extrapolation of the linear portion of the ion signal curve to the $\ln(I_0)$ axis defines a saturation intensity, I_{sat}. Its meaning is nearly independent of the ionization model used. Using the barrier suppression ionization model, I_{sat} can be identified as the critical intensity at which the electron just escapes [i.e., $W(I) = 0$ for $I < I_{\mathrm{sat}}$ and $W(I) = \infty$ for $I > I_{\mathrm{sat}}$]. For the multiphoton ionization model [$W(I) = I^{\sigma n}$] analytical integration of Eq. (1) leads to $I_{\mathrm{sat}} = (\frac{0.56}{\sigma\tau})^{1/n}$, identifying I_{sat} as the intensity where 43% of molecules are ionized. For more complex versions of $W(I)$, I_{sat} is available through numerical integration of Eq. (1).

Figure 2 shows that I_{sat} for benzene is only slightly (by a factor <2) less than that for Xe despite the 3 eV difference in ionization potentials (IP). The relatively high ionization threshold proves to be a general observation for the 23 volatile organic molecules that we have studied. Figure 3 plots I_{sat} as a function of IP for these molecules together with the rare gases. As the solid line in Fig. 3 we show the IP dependence of I_{sat} calculated with $W(I)$ given by ADK tunneling theory. There is good agreement with this quasistatic field ionization model for He, Ne (not included in Fig. 3), and Xe which is expected to provide a lower limit for the ionization rate and consequently an upper limit for I_{sat}. This agreement validates our experimental approach. Of course, it is naive to expect ADK theory to apply to molecules. Figure 3 shows that it *does not even provide an upper bound* for the saturation intensity. For all of the organic molecules studied, we find that

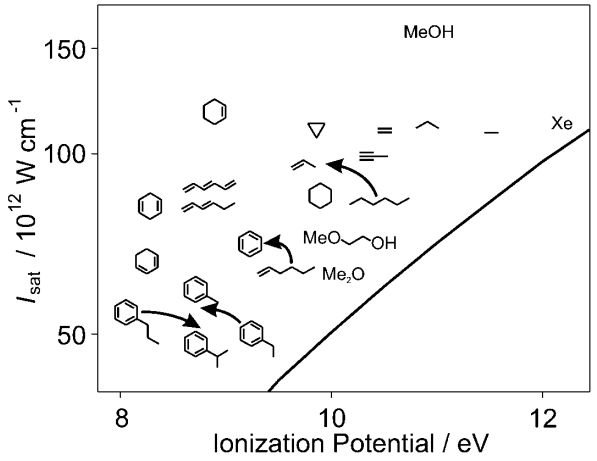

FIG. 3. Saturation intensities, I_{sat} as described in the text, for the series of 23 volatile organic molecules, as a function of the ionization potential of the molecule. The molecules, ethane, ethene, propane, propene, propyne, *cyclo*-propane, hexane, *cyclo*-hexane, hex-1-ene, *cyclo*-hexene, hexa-1,3-diene, *cyclo*-hexa-1,4-diene, hexa-1,3,5-triene, benzene, toluene, ethylbenzene, *n*-propylbenzene, *i*-propylbenzene, 2-methoxyethanol, methanol and dimethylether, and xenon are identified by chemical symbols. Generally the symbols have been centered over the relevant data point. Arrowheads mark the positions of molecules which have been displaced to avoid congestion. The solid curve shows I_{sat}, calculated using ADK tunneling theory.

I_{sat} is greater than that predicted by ADK theory by as much as 5 times. Although it is harder to define a saturation intensity with their focused beam geometry, results similar to ours on much smaller sets of molecules are implicit in the data and the analysis of Chin and co-workers [13,18,19] and Ledingham and co-workers [20]. O_2 and to some extent HCl are the only molecules where suppressed ionization has been remarked on directly [18,21]. The large and varied set of molecules we have studied reveals the generality of this behavior.

There has been a great deal of speculation on the reduced ionization threshold for neutral molecules aligned with the field. Our experiment was not designed to study this directly. However, since it measures absolute rates, it provides a clear limit on possible angle-dependent alignment effects.

Our pulse duration is sufficiently short to ensure that there can be no field induced alignment of the molecules [22] and they are frozen in random orientations for the duration of the ionization pulse. Assuming that the ionization rate is determined by the component of the electric field in the direction of a particular molecular axis, integration over the projection angle yields the intensity dependence of the ion signal under these circumstances, S_{orient}. To model this dependence we have investigated two cases using the barrier suppression ionization model [23], where the integration can be handled analytically. The first case assumes a single active axis so that $W_x(I) \gg W_y(I) \approx W_z(I)$. The second assumes

$W_x(I) = W_y(I) \gg W_z(I)$. In this intermediate case, ionization is caused only by the component of the field in a molecular plane. In both cases, linear behavior with the same slope as the anisotropic case is predicted at high intensity (Fig. 1). Extrapolation back to the $\ln(I_0)$ axis leads to an apparent saturation intensity, I'_{sat}, which is greater than I_{sat}. That is, the measured I'_{sat} would exceed the real but isotropic I_{sat} by 7.4 for the first case and 1.86 in the second. The factor of 7.4 represents an upper limit on the shift that alignment can cause in the saturation intensity.

At first sight this might be taken as sufficient to explain our results. However, alignment also implies a measurable change in the intensity dependence of the ion yield which we do not observe. For a single axis molecule S_{orient} approaches the high intensity asymptote very gradually (Fig. 1, dashed line) so that data collected as high as $10 \times I_{\mathrm{sat}}$ will not come close to the asymptotic region. Our data are sufficiently accurate to ensure that the molecular ion signal has the same limiting slope as Xe and approaches it with similar asymptotic behavior [24]. Therefore, in our experiment, strong angle-dependent ionization can be ruled out for all molecules studied. We do not rule out small differences in I_{sat} for differently oriented molecules. In this case I'_{sat} measures an intermediate value between, at most, relatively similar values of I_{sat}.

In conclusion the high saturation intensities that we find to be typical for organic molecules appear to be typical of many complex media. In fused silica the damage threshold has been found to exceed the tunneling threshold by an order of magnitude [5]. The diatomics O_2 and HCl were found to ionize at higher intensity than would be implied by ADK tunneling calculations [18,21]. Although there are many models for tunnel ionization of neutral molecules [10,13], to our knowledge, this apparently general phenomenon has never been predicted.

*Present address: Department of Physics and Astronomy, University of Glasgow, G12 8QQ, United Kingdom.

[1] P. Lambropoulos, Phys. Rev. Lett. **55**, 2141 (1985).
[2] M. V. Ammosov, N. B. Delone, and V. P. Krainov, Sov. Phys. JETP **64**, 1191 (1986).
[3] B. Walker *et al.*, Phys. Rev. Lett. **73**, 1227 (1994).
[4] J. Tersoff and D. R. Hamann, Phys. Rev. B **31**, 805 (1985).
[5] M. Lenzner *et al.*, Phys. Rev. Lett. **80**, 4076 (1998).
[6] J. J. Macklin, J. D. Kmetec, and C. L. Gordon III, Phys. Rev. Lett. **70**, 766 (1993); J. L. Krause, K. J. Schafer, and K. C. Kulander, Phys. Rev. Lett. **68**, 3535 (1992).
[7] C. Ellert *et al.*, Philos. Trans. R. Soc. London A **356**, 329 (1998).
[8] K. W. D. Ledingham and R. P. Singhal, Int. J. Mass Spectrom. Ion Process. **163**, 149 (1997).
[9] H. D. Beckey, *Field Ionization Mass Spectrometry* (Permagon Press, Oxford, 1971).
[10] M. J. DeWitt and R. J. Levis, J. Chem. Phys. **108**, 7739 (1998); **108**, 7045 (1998); **110**, 11368 (1999); Phys. Rev. Lett. **81**, 5101 (1998); B. S. Prall, M. J. DeWitt, and R. J. Levis, J. Chem. Phys. **111**, 2865 (1999).
[11] M. Lezius *et al.* (to be published).
[12] A. Talebpour, J. Yang, and S. L. Chin, Opt. Commun. **163**, 29 (1999).
[13] A. Talebpour, S. Larochelle, and S. L. Chin, J. Phys. B **31**, 2796 (1998).
[14] A. Talebpour, S. Larochelle, and S. L. Chin, J. Phys. B **31**, L49 (1998).
[15] T. Seideman, M. Y. Ivanov, and P. B. Corkum, Phys. Rev. Lett. **75**, 2819 (1995); E. Constant, H. Stapelfeldt, and P. B. Corkum, Phys. Rev. Lett. **76**, 4140 (1996).
[16] P. Hansch and L. D. Van Woerkom, Opt. Lett. **21**, 1286 (1996).
[17] More rigorously, integration over the temporal pulse shape can be included in the analysis but using an equivalent square pulse proves a reasonable approximation.
[18] A. Talebpour, C. Y. Chien, and S. L. Chin, J. Phys. B **29**, L677 (1996); C. Guo, M. Li, J. P. Nibarger, and G. N. Gibson, Phys. Rev. A **58**, R4271 (1998).
[19] Y. Liang *et al.*, J. Phys. B **30**, 1369 (1997).
[20] K. W. D. Ledingham *et al.*, J. Phys. Chem. A **102**, 3002 (1998); D. J. Smith *et al.*, Rapid Commun. Mass Spectrom. **12**, 813 (1998).
[21] P. Dietrich and P. B. Corkum, J. Chem. Phys. **97**, 3187 (1992).
[22] C. Ellert and P. B. Corkum, Phys. Rev. A **59**, R3170 (1999).
[23] S. Augst *et al.*, Phys. Rev. Lett. **63**, 2212 (1989).
[24] The limiting slope is always established below the Coulomb explosion limit.